

Novel Control Strategy for Modular Multilevel Converters Based on Differential Flatness Theory

Majid Mehrasa, Edris Pouresmaeil, *Senior Member, IEEE*, Shamsodin Taheri, Ionel Vechiu, *Member, IEEE*, João P. S. Catalão, *Senior Member, IEEE*

Abstract—This paper aims to present a novel control strategy for Modular Multilevel Converters (MMC) based on differential flatness theory (DFT), in which instantaneous active and reactive power values are considered as the flat outputs. To this purpose, a mathematical model of the MMC taking into account dynamics of the ac-side current and the dc-side voltage of the converter is derived in a d-q reference frame. Using this model, the flat outputs-based dynamic model of MMC is obtained to reach the initial value of the proposed controller inputs. In order to mitigate the negative effects of the input disturbance, model errors, and system uncertainties on the operating performance of the MMC, the integral-proportional terms of the flat output errors are added to the initial inputs. This can be achieved through defining a control Lyapunov function which can ensure the stability of the MMC under various operating points. Moreover, the small-signal linearization method is applied to the proposed flat output-based model to separately evaluate the variation effects of controller inputs on flat outputs. The proficiency of the proposed method is researched via MATLAB simulation. Simulation results highlight the capability of the proposed controller in both steady-state and transient conditions in maintaining MMC currents and voltages, through managing active and reactive power.

Index Terms—Modular Multilevel Converter (MMC), differential flatness theory (DFT), active and reactive power.

I. NOMENCLATURE

Indices

i	1,2
j	1,2
k	a,b,c

J.P.S. Catalão and E. Pouresmaeil acknowledge the support by FEDER funds through COMPETE 2020 and by Portuguese funds through FCT, under Projects SAICT-PAC/0004/2015 - POCI-01-0145-FEDER-016434, POCI-01-0145-FEDER-006961, UID/EEA/50014/2013, UID/CEC/50021/2013, UID/EMS/00151/2013, and SFRH/BPD/102744/2014, and also funding from the EU 7th Framework Programme FP7/2007-2013 under GA no. 309048.

M. Mehrasa is with C-MAST, University of Beira Interior, Covilhã 6201-001, Portugal (m.majidmehrassa@gmail.com).

E. Pouresmaeil is with INESC-ID, Instituto Superior Técnico, University of Lisbon, Lisbon 1049-001, Portugal, and also with ESTIA Institute of Technology, ESTIA, F-64210, Bidart, France (edris.pouresmaeil@gmail.com).

S. Taheri is with Université du Québec en Outaouais, Gatineau, Canada (e-mail: shamsodin.taheri@uqo.ca).

I. Vechiu is with ESTIA Institute of Technology, ESTIA, F-64210, Bidart, France (e-mail: i.vechiu@estia.fr)

J.P.S. Catalão is with INESC TEC and the Faculty of Engineering of the University of Porto, Porto 4200-465, Portugal, also with C-MAST, University of Beira Interior, Covilhã 6201-001, Portugal, and also with INESC-ID, Instituto Superior Técnico, University of Lisbon, Lisbon 1049-001, Portugal (e-mail: catalao@ubi.pt).

Abbreviation

MMC	Modular Multilevel Converter
SLPWM	Shifted Level Pulse Width Modulation
DFT	Differential Flatness Theory
SM	Sub-Modules
PCC	Point of Common Coupling
KVL	Kirchhoff's Voltage Law
KCL	Kirchhoff's Current Law

Variables

i_k	Output Currents of MMC
i_{uk}	Upper's arm Currents of MMC
i_{lk}	Lower's arm Currents of MMC
$i_{cir k}$	Circulating Currents of MMC
i_{dq}	Output Currents of MMC in d-q reference frame
$i_{cir 0}$	Circulating Currents of MMC in 0dq reference frame
v_{dc}	Dc link voltage of MMC
v_{uk}	Upper's SM voltages of MMC
v_{lk}	Lower's SM voltages of MMC
u_k	The control factors of MMC
u_{dq}	The control factors of MMC in d-q reference frame
v_k	PCC voltages
v_m	The maximum magnitude of PCC voltages
v_{dq}	PCC voltages in d-q reference frame
P	Instantaneous active power of MMC
Q	Instantaneous reactive power of MMC
y_{12}	Flat Outputs
x_{123}	The state variables
u_{12}	The control inputs
e_{i1}	The proportional errors of the flat outputs
e_{i2}	The integral errors of the flat outputs
Δy_i	The perturbations of flat outputs
Δu_i	The perturbations of control inputs

Parameters

L	Output inductance of MMC
R	Output resistance of MMC
L_t	Arm's inductance of MMC
R_t	Arm's resistance of MMC
C_f	AC Filter Capacitor
C_{dc}	dc-link Capacitor
N	Sub modules numbers in per arm

II. INTRODUCTION

High-power and Medium-voltage power electronics-based converters have been continuously employed in high-technology industries, traction systems and regenerative energy sources, since they offer effective power structures, flexible designed controllers, various dynamic models, and effective pulse-width-modulation (PWM) techniques [1-4]. These features can lead to low harmonic components, fast responses against dynamic changes, improved power factors as well as power quality in grid-connected systems, not to mention a ride-through capability and/or a redundant converter design in various operating conditions [5-7]. Among existing power electronic-based converters, modular multilevel converters (MMCs) have been gaining popularity due to their full modularity and easy extend ability to meet different voltage and power level requirements in various applications i.e., photovoltaic systems, large wind turbines, ac motor drives, HVDC systems, dc-dc transformers, battery electric vehicles, distributed energy resources (DERs), and flexible alternating current transmission systems (FACTS) [8-13].

However, the MMCs commonly demand complex control configurations in comparison with other converter topologies. Therefore, designing an appropriate control technique for the control and operation of the MMC in power systems is essential. To this end, several studies in the literature have addressed the control concept of the MMCs in power systems which will be briefly presented as follows [14-24]. A nearest level control (NLC) along with an optimized control strategy is proposed to govern the MMC operation in [14], which is based on the dynamic redundancy and the utilization ratio of the sub-modules. A model predictive direct current control is provided for the MMC in [15]. The proposed control technique can maintain the load current within strict bounds around sinusoidal references and minimize capacitor voltage changes and circulating currents. In recent years, dynamic models for MMCs have been the topics of several works [16-18]. In [18], a new switching-cycle state-space model is designed for a MMC in which a respective switching-cycle control approach is also proposed by considering the unused switching states of the converter. Through using the average voltage of all the sub-modules (SMs) in each control cycle, a fast voltage-balancing control along with a numerical simulation model are proposed for the MMC in [19]. The sinusoidal common-mode (CM) voltage and circulating currents are employed for designing various control techniques in MMCs. In fact, in order to attenuate the low-frequency components of the SM capacitor voltage, the sinusoidal common-mode voltage and circulating current are used to design a control strategy for the MMC in [20]. In [21], optimized sinusoidal CM voltage and circulating current are used to limit the SM capacitor voltage ripple and the peak value of the arm current. Also, for adjustable-speed drive (ASD) application under constant torque low-speed operation, two control techniques based on injecting a square-wave CM voltage on the ac-side and a circulating current are proposed to reduce the magnitude of the SM capacitor voltage ripple [22]. Furthermore, a control strategy based on a sinusoidal CM voltage and circulating current is proposed for an MMC-based

ASD over the complete operating speed region [23]. In addition, the peak value of the sinusoidal common mode voltage can be a key solution for analyzing the SM capacitor voltage ripple [24].

In this paper, a novel control strategy based on differential flatness theory (DFT), inspired by that was used for the control of converters in [25-27], is presented to control the operation of MMC in power systems. The flat outputs required for the DFT-based control technique are the instantaneous active and reactive power of the MMC. The initial values of the proposed controller inputs can be driven by a new dynamic equation of the MMC, achieved as per the flat outputs. Then, a control Lyapunov function based on the respective integral-proportional errors of flat output is utilized to provide a stable operation against input disturbance, model errors, and system uncertainties. Also, in order to evaluate the variation effects of controller inputs on flat outputs, the relevant transfer functions are obtained through the small signal model of the flat outputs-based dynamic equations. In comparison with other existing control techniques for MMC, the proposed controller exhibits several considerable advantages in terms of the stability issues for robustness enhancement, highly improvements of MMC power sharing ability, less overshoot and undershoot for SM voltages and transient through considering simultaneously all the input disturbance, model errors, and system uncertainties and applying directly the MMC active and reactive power as the state variables. The simulation analysis using Matlab/Simulink clearly demonstrates the effectiveness of the DFT-based control strategy in the proposed MMC-based model under different operating modes.

III. PROPOSED CONTROL TECHNIQUE

Fig. 1 depicts a circuit diagram of the proposed MMC-based model. The MMC consists of six sub-modules in series in each upper and lower arm. Each sub-module can be modeled as a half-bridge IGBT-diode switch-based rectifier.

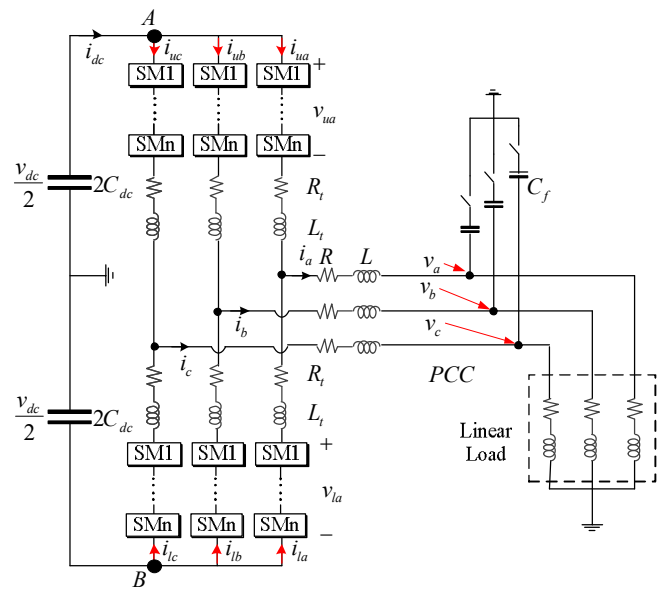


Fig.1. The circuit diagram of the proposed MMC-based model

Two resistance-inductance loads are connected to the PCC in which the second load enters in operating mode by means of the switch at a determined time. Also, a capacitor filter is considered at the PCC of the MMC to improve output ac voltages. Since the dynamic equations of the proposed model are considered in the design of the proposed control strategy; thus, these basic equations as well as a new dynamic model based on the outputs of DFT are extracted in this section.

A. Dynamic analysis of the proposed MMC-based model

As can be seen in Fig. 1, the series connection of sub-modules in both upper and lower arms of the MMC are represented by the controllable voltage sources of v_{uk} and v_{lk} respectively.

These voltages play a key role in controlling the MMC in different operating conditions. As per Fig. 1, the relationships between arm's currents and ac voltages of the MMC, taking into account the dc-link voltage and controllable voltage sources, can be expressed as,

$$v_k + L \frac{di_k}{dt} + Ri_k + L_t \frac{di_{uk}}{dt} + R_t i_{uk} - \frac{v_{dc}}{2} + v_{uk} = 0 \quad (1)$$

$$v_k + L \frac{di_k}{dt} + Ri_k + L_t \frac{di_{lk}}{dt} + R_t i_{lk} + \frac{v_{dc}}{2} - v_{lk} = 0 \quad (2)$$

By summing (1) and (2), the basic dynamic model of the proposed MMC-based model can be obtained as,

$$\left(\frac{2L + L_t}{2} \right) \frac{di_k}{dt} + \left(\frac{2R + R_t}{2} \right) i_k + u_k + v_k = 0 \quad (3)$$

where $i_{uk} + i_{lk} = i_k$. The control factor of u_k is equal to $u_k = (v_{uk} - v_{lk}) / 2$ which reflects the effect of both controllable voltage sources. In addition, the dc-link voltage term is eliminated in (3). By applying KCL's law in the determined points of A and B in Fig.1, the relationships between the MMC's arm currents and the dc-link voltage are stated respectively as,

$$C_{dc} \frac{dv_{dc}}{dt} = -(i_{ua} + i_{ub} + i_{uc}) \quad (4)$$

$$C_{dc} \frac{dv_{dc}}{dt} = (i_{la} + i_{lb} + i_{lc}) \quad (5)$$

Considering circulating currents as $i_{cir} = (i_{uk} - i_{lk}) / 2 - i_{dc} / 3$ and summing up equations (4) and (5), the dynamic equation of dc-link voltage can be obtained as,

$$C_{dc} \frac{dv_{dc}}{dt} + i_{cira} + i_{cirb} + i_{circ} + i_{dc} = 0 \quad (6)$$

Thus, the dynamics of the proposed MMC in the abc reference frame can be obtained as (7),

$$\begin{bmatrix} \left(\frac{2L + L_t}{2} \right) \frac{di_a}{dt} \\ \left(\frac{2L + L_t}{2} \right) \frac{di_b}{dt} \\ \left(\frac{2L + L_t}{2} \right) \frac{di_c}{dt} \\ C_{dc} \frac{dv_{dc}}{dt} \end{bmatrix} = \begin{bmatrix} -\left(\frac{2R + R_t}{2} \right) & 0 & 0 & 0 & 0 & 0 \\ 0 & -\left(\frac{2R + R_t}{2} \right) & 0 & 0 & 0 & 0 \\ 0 & 0 & -\left(\frac{2R + R_t}{2} \right) & 0 & 0 & 0 \\ 0 & 0 & 0 & 0 & -1 & -1 \end{bmatrix} \begin{bmatrix} i_a \\ i_b \\ i_c \\ i_{cra} \\ i_{cirb} \\ i_{cra} \end{bmatrix} + \begin{bmatrix} u_a \\ u_b \\ u_c \\ v_{dc} \\ 0 \end{bmatrix} \quad (7)$$

The park transformation matrix is considered as,

$$\begin{bmatrix} m_d \\ m_q \\ m_0 \end{bmatrix} = \frac{2}{3} \begin{bmatrix} \cos(\omega t) & \cos(\omega t - 2\pi/3) & \cos(\omega t + 2\pi/3) \\ -\sin(\omega t) & -\sin(\omega t - 2\pi/3) & -\sin(\omega t + 2\pi/3) \\ 1/2 & 1/2 & 1/2 \end{bmatrix} \begin{bmatrix} m_a \\ m_b \\ m_c \end{bmatrix} \quad (8)$$

In (8), the variables of 'm' represent all state variables of the proposed MMC. By applying the Park transformation matrix of (8) to (7), the basic dynamic model of the proposed MMC-based model in d-q frame is driven as,

$$\left(\frac{2L + L_t}{2} \right) \frac{di_d}{dt} + \left(\frac{2R + R_t}{2} \right) i_d - \omega \left(\frac{2L + L_t}{2} \right) i_q + u_d + v_d = 0 \quad (9)$$

$$\left(\frac{2L + L_t}{2} \right) \frac{di_q}{dt} + \left(\frac{2R + R_t}{2} \right) i_q + \omega \left(\frac{2L + L_t}{2} \right) i_d + u_q + v_q = 0 \quad (10)$$

$$C_{dc} \frac{dv_{dc}}{dt} + \sqrt{3} i_{cir0} + i_{dc} = 0 \quad (11)$$

Equations (9)-(11) present a basic dynamic model of the MMC-based model. These equations are used to propose the new dynamic model utilized to project the DFT-based control technique and to evaluate the variation effects of controller inputs on flat outputs.

B. The proposed DFT-Based Control Technique

The DFT as an effective nonlinear approach is used to design an appropriate controller to represent the nonlinear properties of the proposed MMC-based model [25-28]. Flatness properties were firstly introduced by Fliess et al. [28]. A nonlinear system can be called as a flat one if all state variables, control inputs and a finite number of the control inputs time derivatives of the nonlinear system can be stated based on the system outputs without any integration [25]. For this flat system, the outputs are considered as the flat outputs. In the next consequence, the output variables of the flat system should be achieved as functions of the state variables, the input variables, and a finite number of their time derivatives. The mathematical description of a flat system can be explained as follows. Considering the general form of the system as (12),

$$\dot{x} = f(x, u) \quad (12)$$

$$y = h(x, u)$$

$$\text{Based on the flat definition, (13) should be governed as,} \\ y = g(x, u, \dot{u}, \ddot{u}, \dots, u^{(2)}) \quad (13)$$

$$\text{Also, another property of a flat system can be written as,} \\ x = \psi(y, \dot{y}, \ddot{y}, \dots, y^{(x)}) \quad (14)$$

$$y = \phi(y, \dot{y}, \ddot{y}, \dots, y^{(x)}) \quad (15)$$

Based on these aforementioned descriptions, defining appropriate flat outputs, control inputs and state variables of the proposed model as the basic requirements of the DFT is firstly considered as follows. According to the basic dynamic model of the MMC, the DFT variables are given as,

$$\begin{aligned} y &= [y_1 \quad y_2] = [P \quad Q] \\ u &= [u_1 \quad u_2] = [u_d \quad u_q] \\ x &= [x_1 \quad x_2 \quad x_3] = [i_d \quad i_q \quad v_{dc}] \end{aligned} \quad (16)$$

Based on (16), the instantaneous active and reactive power of MMC is determined as flat outputs. The relations between flat outputs and MMC state variables can be expressed as,

$$x_1 = \psi(y_1) = \frac{y_1}{v_d}, x_2 = \psi(y_2) = \frac{y_2}{-v_d} \quad (17)$$

According to DFT properties, the proposed MMC-based model is flat, if a set of state variables, so-called flat outputs, from its dynamic model can be found. Therefore, the differential part of the flat output can be expressed by determined state variables and control inputs without any integration. Thus, through equations (9), (10), and (17), the dynamic representation of specified flat outputs in the proposed control technique can be achieved as,

$$\begin{aligned} \frac{dy_1}{dt} &= \dot{v}_d x_1 - \left(\frac{2R+R_t}{2L+L_t} \right) v_d x_1 + \omega v_d x_2 - \left(\frac{2}{2L+L_t} \right) v_d u_1 \\ &- \left(\frac{2}{2L+L_t} \right) v_d^2 \end{aligned} \quad (18)$$

$$\begin{aligned} \frac{dy_2}{dt} &= \dot{v}_d x_2 - \left(\frac{2R+R_t}{2L+L_t} \right) y_2 + \omega y_1 + \left(\frac{2}{2L+L_t} \right) v_d u_2 \\ &- \left(\frac{2}{2L+L_t} \right) v_d^2 \end{aligned} \quad (19)$$

Equations (17), (18) and (19) are used to attain the initial values of the control technique inputs as,

$$\begin{aligned} u_1 &= \left(\frac{2L+L_t}{2} \right) \frac{\dot{v}_d y_1}{v_d^2} - \left(\frac{2R+R_t}{2} \right) \frac{y_1}{v_d} - \left(\frac{2L+L_t}{2} \right) \frac{\omega y_2}{v_d} \\ &- v_d - \left(\frac{2L+L_t}{2v_d} \right) \dot{y}_1 \end{aligned} \quad (20)$$

$$\begin{aligned} u_2 &= \left(\frac{2L+L_t}{2v_d} \right) \dot{y}_2 - \left(\frac{2L+L_t}{2} \right) \frac{\dot{v}_d y_2}{v_d^2} + \left(\frac{2R+R_t}{2} \right) \frac{y_2}{v_d} \\ &- \left(\frac{2L+L_t}{2} \right) \frac{\omega y_1}{v_d} \end{aligned} \quad (21)$$

In order to obtain a robust control system against the input disturbance, model errors, and system uncertainties, proportional-integral errors of the flat outputs are defined as,

$$e_{i1} = y_i^* - y_i, e_{i2} = \int_0^t (y_i^*(h) - y_i(h)) dh \quad (22)$$

The flat output errors are entirely considered through e_{i1} and e_{i2} that can lead to designing a proper controller for decreasing the various errors of MMC active and reactive power sharing. The effects of the flat output errors on the proposed control inputs can be specified by the stability evaluation of the following Lyapunov function as,

$$E(e_{i1}, e_{i2}, e_{21}, e_{22}) = \frac{1}{2} e_{i1}^2 + \frac{1}{2} e_{i2}^2 + \frac{1}{2} e_{21}^2 + \frac{1}{2} e_{22}^2 \quad (23)$$

The accurate operation of DFT with approaching the flat output errors to zero can be guaranteed by stability analysis of (23). The derivative of (23) is driven as,

$$\begin{aligned} \dot{E}(e_{i1}, e_{i2}, e_{21}, e_{22}) &= e_{i1} \dot{e}_{i1} + e_{i2} \dot{e}_{i2} + e_{21} \dot{e}_{21} + e_{22} \dot{e}_{22} \\ &= e_{i1} \dot{e}_{i1} + e_{i2} \dot{e}_{i2} + e_{21} \dot{e}_{21} + e_{22} \dot{e}_{22} \end{aligned} \quad (24)$$

Equations (22) and (24) can be rewritten based on (18) and (19), as follows,

$$\begin{aligned} \dot{E}(e_{i1}, e_{i2}, e_{21}, e_{22}) &= e_{i1} \left(\dot{y}_1^* - \dot{v}_d x_1 + \left(\frac{2R+R_t}{2L+L_t} \right) y_1 + \omega y_2 \right. \\ &\left. + \left(\frac{2}{2L+L_t} \right) v_d u_1 + \left(\frac{2}{2L+L_t} \right) v_d^2 + e_{i2} \right) \\ &+ e_{i2} \left(\dot{y}_2^* + \dot{v}_d x_2 + \left(\frac{2R+R_t}{2L+L_t} \right) y_2 - \right. \\ &\left. \omega y_1 - \left(\frac{2}{2L+L_t} \right) v_d u_2 + e_{22} \right) \end{aligned} \quad (25)$$

By making flat outputs-based Lyapunov function globally asymptotically stable, (25) leads to the proposed control inputs as,

$$u_1 = \frac{2L+L_t}{2v_d} \times \left(-\dot{y}_1^* + \dot{v}_d x_1 - \left(\frac{2R+R_t}{2L+L_t} \right) y_1 - \omega y_2 \right. \\ \left. - \left(\frac{2}{2L+L_t} \right) v_d^2 + e_{i2} + \lambda_1 e_{i1} \right) \quad (26)$$

$$u_2 = \frac{2L+L_t}{2v_d} \times \left(\dot{y}_2^* + \dot{v}_d x_2 + \left(\frac{2R+R_t}{2L+L_t} \right) y_2 - \omega y_1 \right. \\ \left. + e_{22} + \lambda_2 e_{21} \right) \quad (27)$$

The proposed control inputs of (26) and (27) lead to the global asymptotic stability of flat outputs errors-based Lyapunov function as,

$$\dot{E}(e_{i1}, e_{i2}, e_{21}, e_{22}) = -\lambda_1 e_{i1}^2 - \lambda_2 e_{21}^2 \leq 0 \quad (28)$$

Equation (28) verifies that the designed closed-loop control technique driven from (26) and (27) can provide a stable operation of the proposed MMC-based model. The block diagram of the proposed control technique is presented in Fig.2. The flat outputs errors and their integral are calculated from the measured instantaneous active and reactive power and the desired values of instantaneous power of the MMC as depicted in the block diagram. In order to reach global results for the proposed DFT based controller, $v_d = v_d^*$ for the term of \dot{v}_d and consequently $\dot{v}_d = 0$.

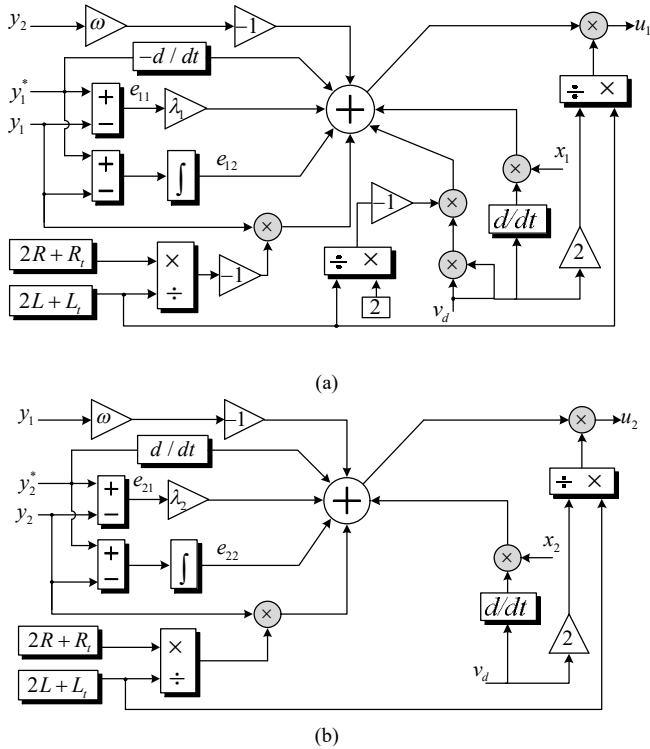


Fig. 2. The proposed control technique of DFT (a) the component of u_1 (b) the component of u_2 .

IV. EFFECTS OF THE CONTROL INPUTS PERTURBATION

The MMC control inputs u_1 and u_2 aim to provide accurate tracking for the flat outputs. Thus, the MMC operation through presenting suitable active and reactive power sharing is highly dependent on the control inputs. The effects of control input variations on the flat outputs are investigated in this section. By applying (17) to (18) and (19) and using the small signal linearization technique, the relations between the perturbations of flat outputs and control inputs can be achieved as,

$$\Delta y_1 = F_{11}(s)\Delta u_1 + F_{12}(s)\Delta u_2 \quad (29)$$

$$\Delta y_2 = F_{21}(s)\Delta u_1 + F_{22}(s)\Delta u_2 \quad (30)$$

The transformation functions ($F_{ij}(s)$) presented in (29) and (30) are defined as,

$$F_{11}(s) = \frac{-\left(s - \frac{\dot{v}_d}{v_d} + \left(\frac{2R+R_t}{2L+L_t}\right)\right)\left(\frac{2}{2L+L_t}\right)v_d}{\Delta}$$

$$F_{12}(s) = \frac{-\omega\left(\frac{2}{2L+L_t}\right)v_d}{\Delta}, \quad F_{21}(s) = \frac{\omega\left(\frac{2}{2L+L_t}\right)v_d}{\Delta} \quad (31)$$

$$F_{22}(s) = \frac{-\left(s - \frac{\dot{v}_d}{v_d} + \left(\frac{2R+R_t}{2L+L_t}\right)\right)\left(\frac{2}{2L+L_t}\right)v_d}{\Delta}$$

where the term of Δ in (31) is equal to,

$$\Delta = s^2 + 2\left(-\frac{\dot{v}_d}{v_d} + \left(\frac{2R+R_t}{2L+L_t}\right)\right)s + \left(-\frac{\dot{v}_d}{v_d} + \left(\frac{2R+R_t}{2L+L_t}\right)\right)^2 - \omega^2 \quad (32)$$

Each transformation function of $F_{ij}(s)$ is used to show the effect of the control inputs on their respective flat outputs. Furthermore, based on equations (29) and (30), each of flat outputs is affected by both control inputs. The Bode diagram is used to evaluate the impact of each control input on the flat outputs when the perturbation is being increased. The MMC parameters given in Table I, are used in this section. The effects of the control inputs are separately considered as,

$$\Delta y_{11} = \Delta y_1 \Big|_{\Delta u_2=0} = F_{11}(s)\Delta u_1,$$

$$\Delta y_{12} = \Delta y_1 \Big|_{\Delta u_1=0} = F_{12}(s)\Delta u_2$$

$$\Delta y_{21} = \Delta y_2 \Big|_{\Delta u_2=0} = F_{21}(s)\Delta u_1,$$

$$\Delta y_{22} = \Delta y_2 \Big|_{\Delta u_1=0} = F_{22}(s)\Delta u_2 \quad (33)$$

Fig. 3 shows the Bode diagram of the proposed flat outputs with the perturbation variations of the first control input. As it can be seen from this figure, an increase in the perturbation of the first control input impacts on the second flat output is more considerable than that on the first flat output. It means that the perturbation of the first control input can lead to a significant deviation of the second flat output from its desired value during the MMC operation. The perturbation effect of the second control input is examined in Fig. 4. As can be seen from the curves in Fig. 4, in comparison with the second flat output, the first flat output is significantly affected by the perturbation variations of the second control input.

V. SIMULATION RESULTS

To verify the effectiveness of the proposed control technique, a detailed model of the aforementioned system as summarized in Fig. 5 is implemented in the Matlab/Simulink. It is worth mentioning that the discrete mode with a sample time of 50 microsec is selected to execute the simulation of the MMC-based model in the Matlab environment. In order to assess the performance of the proposed technique, a load step change is applied to the system. Initially, in the steady state condition the MMC is regulated to provide the required power of 5.5MW+j2MVAR for a RL load. Then, in the load variation state, it is stepped up to 10 MW+j5MVAR.

A. Control Technique Effect Assessment

To assess the capability of the proposed DFT in a steady-state operation of the MMC, two time intervals are considered in this subsection. The first load, given in table I, is used in both operating conditions. In the first interval from 0 to 0.4, the control technique is applied to the MMC resulting in a stable voltage as shown in Fig. 6. Then, at $t=0.4$ s, the designed control method is removed from the MMC. In consequence of the controller absence, the MMC SM voltages deviate from their desired values as depicted in Fig. 7. In fact, the lack of the proposed control technique leads to an unbalanced and unstable voltage at PCC. Fig. 8 and Fig. 9 show the corresponding active and reactive power sharing

among the MMC, load and capacitor filter. According to these figures, after removing the proposed control technique, all active and reactive power experience severe transient responses with high fluctuations, unable to track their reference values.

B. Load Variation Evaluation

To evaluate the dynamic operation of the proposed control technique during transient state due to changes in loads connected to the PCC, MMC variables consisting of the flat outputs, output and SM voltages are taken into account. The proposed MMC model parameters for relevant loads are given in Table I.

Fig. 10 shows the SM's voltages of the phase "a" for a load change at $t=0.4s$. It can be seen that in spite of the load change the upper and lower SM's voltages maintain their reference values after a short transient period. In addition, the PCC voltage of phase "a" is illustrated in Fig. 11. According to this simulation result, the proposed MMC model performs properly to maintain the output AC voltage regardless of the slight undershoot and overshoot due to a load variation at the starting point.

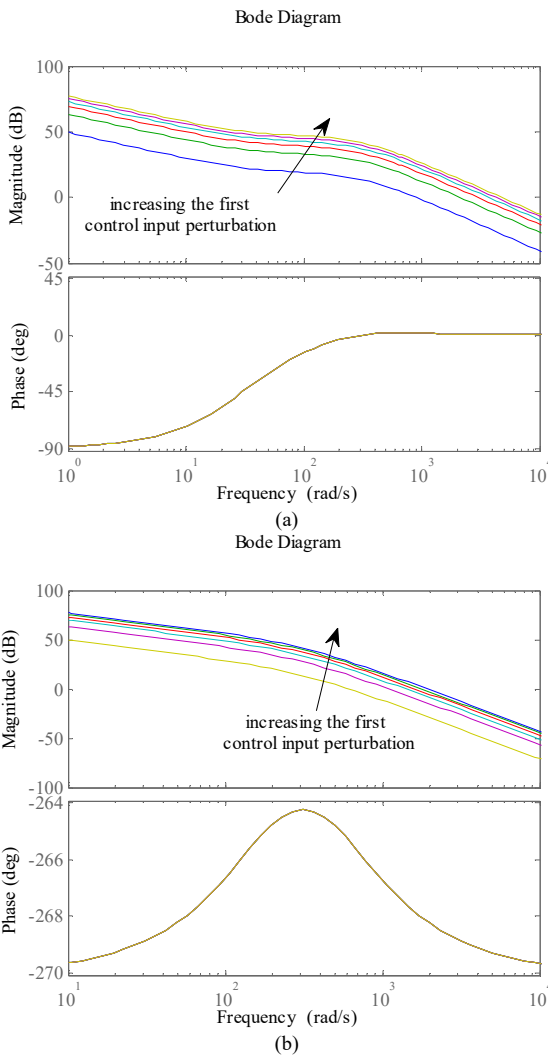


Fig. 3. The perturbation effect of first control input on (a) the first flat output (b) the second flat output.

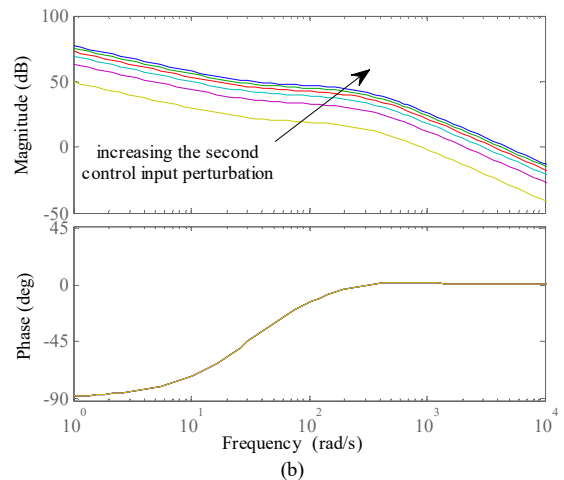
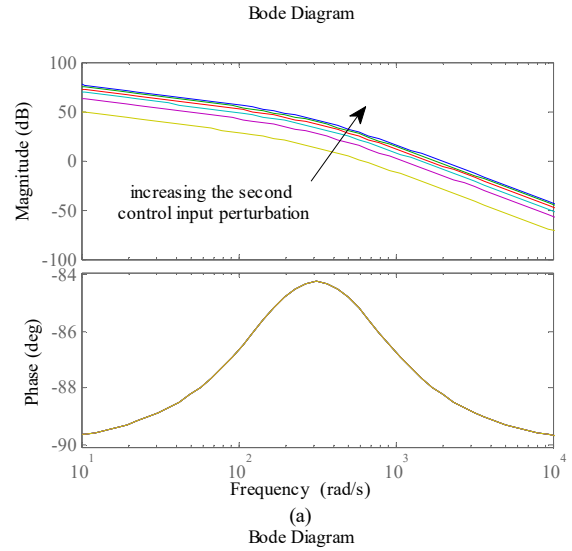


Fig. 4. The effects of second control inputs on (a) the first flat output (b) the second flat output.

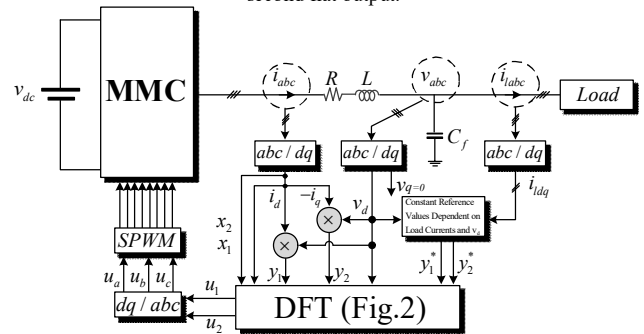


Fig. 5. The single diagram of simulated model.

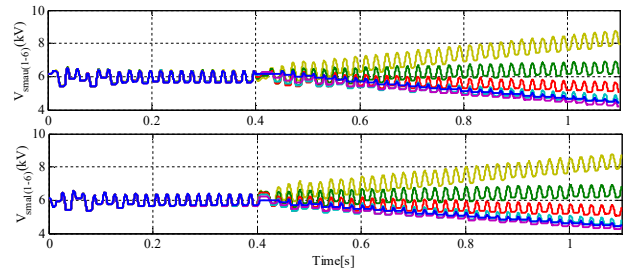


Fig. 6. SM's voltages of MMC.

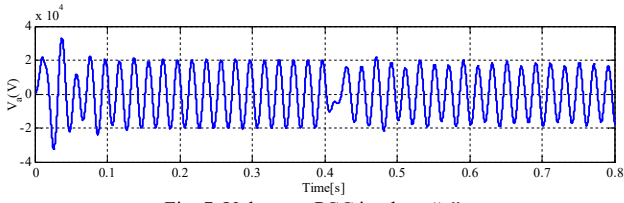


Fig. 7. Voltage at PCC in phase "a".

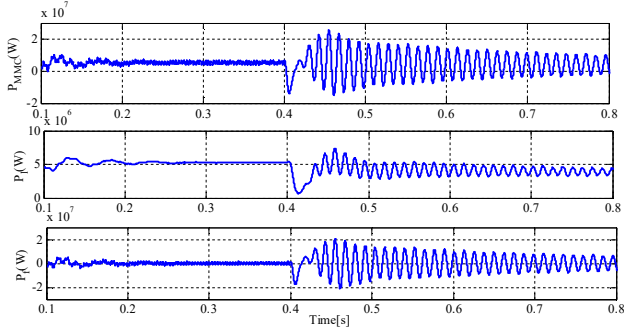


Fig. 8. Active power of MMC, load and AC filter.

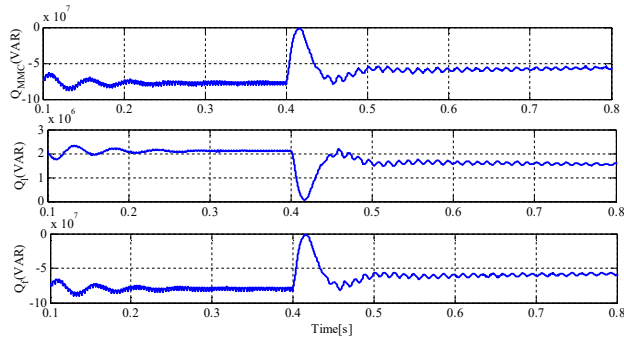


Fig. 9. Reactive power of MMC, load and AC filter.

TABLE I

THE PROPOSED MMC MODEL SPECIFICATIONS WITH RELATED LOADS

L_l (mH)	20	N	6
L (mH)	45	f (Hz)	50
R_l (Ω)	1	Load Active Power I	5.5MW
R (Ω)	0.1	Load Reactive Power I	2MVAR
v_{dc} (V)	36000	Load Active Power II	4.5MW
v_m (V)	20000	Load Reactive Power II	3MVAR

The flat outputs including active and reactive power values are shown in Fig. 12 and Fig. 13. In steady state operation, the active power of the MMC follows properly the active power of load and the AC filter capacitor as depicted in Fig. 12. Moreover, it can be seen from the responses during the time interval of [0.4, 0.8] that the proposed control technique is able to maintain the stability of the active power of the MMC after a short transient period. The MMC reactive power performance as the second flat output is evaluated in Fig. 13. The reactive power demanded from the load to maintain PCC voltages can be appropriately provided by the proposed MMC model through the AC filter capacitor.

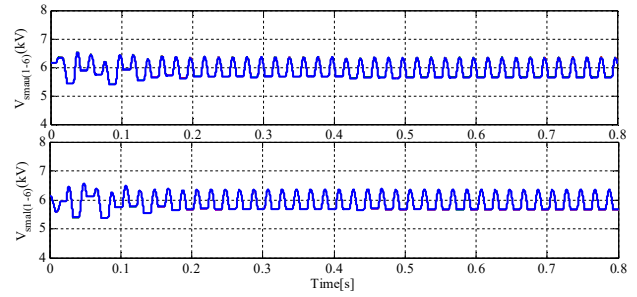


Fig. 10. SM's voltages of MMC with load variations at t=0.4 s.

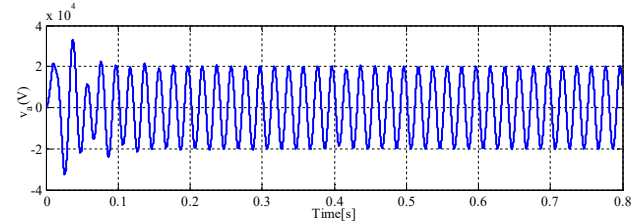


Fig. 11. PCC voltage of phase "a" with load variations at t=0.4 s.

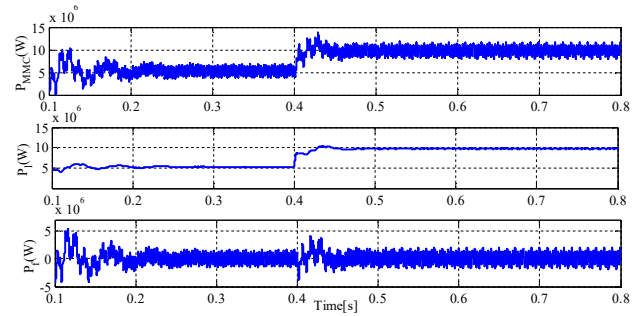


Fig. 12. Active power of MMC, load and AC filter with load variations at t=0.4 s.

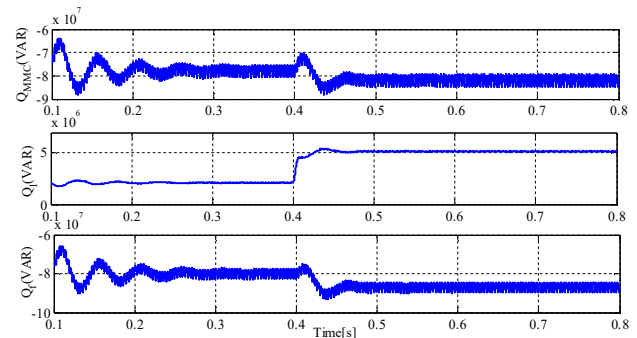


Fig. 13. Reactive power of MMC, load and AC filter with load variations at t=0.4 s.

C. Parameters Variation Evaluation

As discussed earlier, the proposed control technique can operate well under parameter variations. As per the MMC parameter patterns in both states presented in Table I and Table II, SM's voltages of the MMC can be satisfied as shown in Fig. 14. It should be noted that although the SM's voltages experience an undershoot immediately after parameters variation time, the reference values of this voltage can be followed by the MMC after a short transient period.

This confirms approaching the negative effects of the parameter variation to zero. While parameters variation takes place, the output voltage of MMC in phase "a" is involved

with a short transient time as shown in Fig. 15. Then, a sinusoidal pure waveform is achieved for MMC output voltage due to the stable operation of the proposed control technique.

As renewable energy systems are expected to make a significant contribution to supply worldwide electricity in a more secure and economic way, it is essential to carry on verifying the effectiveness of control systems under the condition that there is an imbalance the generated and the consumed power. This research may be regarded as a basis for the development of modular multilevel converters and controllers in grid-connected systems to provide a long-term energy security.

To evaluate the ability of the proposed MMC-based model at reaching the desired value of its flat outputs under parameter variations, following scenario is given through Fig. 16 and Fig. 17. The MMC first operates in a steady state in which the MMC and the load active power approach to its target values. Then, after a parameter variation, the active power of the MMC, introduced as the first flat output experiences temporal fluctuations which will be attenuated after some short time cycles. In fact, the proposed control technique offers stable active power for the MMC, the load and the AC filter capacitor. In addition, the proposed technique contributes to provide the reactive power known as the second flat output of the MMC even parameter variation happens. As can be seen from Fig. 17, the transient waveforms of the load and MMC reactive power during parameters variation can be damped and subsequently the desired reactive power can be achieved.

TABLE II
THE SECOND PARAMETERS FOR THE PROPOSED MMC MODEL

$L_{i2}(mH)$	35	$R_{i2}(\Omega)$	2.5
$L_2(mH)$	30	$R_2(\Omega)$	0.22

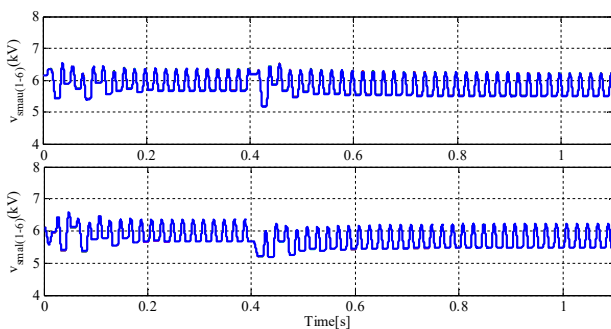


Fig. 14. SM's voltages of MMC with parameters variations at $t=0.4$ s.

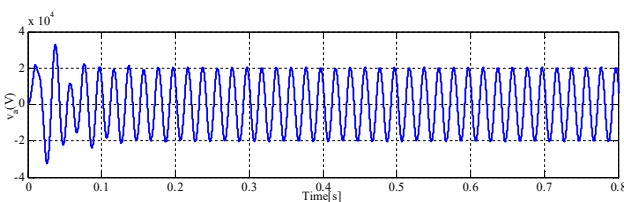


Fig. 15. PCC voltage of phase "a" with parameters variations at $t=0.4$ s.

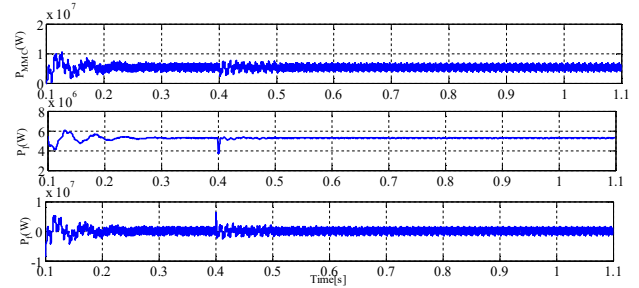


Fig. 16. Active power of MMC, load and AC filter with parameters variations at $t=0.4$ s.

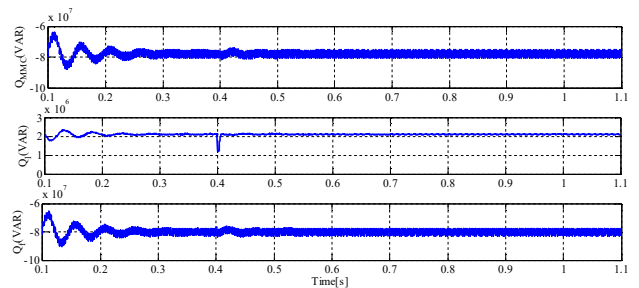


Fig. 17. Reactive power of MMC, load and AC filter with parameters variations at $t=0.4$ s.

VI. CONCLUSION

This paper addressed the differential flatness theory (DFT), used to control a modular multilevel converter (MMC), as a new contribution to earlier studies. Using the basic dynamic model of MMC in a d-q reference frame as well as defining appropriate flat outputs, new flat outputs-based dynamic equations were achieved. Then, these equations were used to obtain an initial value for controller inputs. In order to guarantee the stable operation of the MMC against the input disturbance, model errors, and system uncertainties, a control Lyapunov function based on integral-proportional errors of the flat output was employed. In addition, the small-signal model of the flat outputs-based dynamic equation was developed and then the variation effects of controller inputs on flat outputs were accurately assessed. To evaluate the effectiveness of the proposed DFT-based control technique, Matlab simulations were carried out under challenging conditions, namely variations in parameters and load. The simulation results validated that the proposed control technique upholds the voltage levels accurately through providing active and reactive power. Overall, this novel DFT-based control scheme offered an efficient control design which can be upgraded to a varied range of complex converter topologies used for renewable energy applications.

REFERENCES

- [1] E. Pournesmaeil, M. Mehra, M.A. Shokridehaki, E.M.G Rodrigues, and J.P.S Catalão, "Control of Modular Multilevel Converters for Integration of Distributed Generation Sources into the Power Grid," *IEEE SEGE*, pp.1-6, Nov. 2015.
- [2] F. Ma, Q. Xu, Z. He, C. Tu, Z. Shuai, A. Luo, and Y. Li, "A Railway Traction Power Conditioner Using Modular Multilevel Converter and Its Control Strategy for High-Speed Railway System," *IEEE Transactions on Transportation Electrification*, vol. 2, no. 1, pp. 96 – 109, Jan. 2016.
- [3] D. Montesinos-Miracle, M. Massot-Campos, J. Bergas-Jane, S. Galceran-Arellano, and A. Rufer, "Design and Control of a Modular Multilevel DC/DC Converter for Regenerative Applications," *IEEE Trans. on Power Electronics*, vol. 28, no. 8, pp. 3970 – 3979, Aug. 2013.

[4] A.A Gebreel and L. Xu, "DC-AC Power Conversion Based on Using Modular Multilevel Converter With Arm Energy Approximation Control," *IEEE Power and Energy Tech. Sys.*, vol. 3, no. 2, pp. 32 – 42, June 2016.

[5] D. Wu and L. Peng, "Analysis and Suppressing Method for the Output Voltage Harmonics of Modular Multilevel Converter," *IEEE Trans. on Power Electron.*, vol. 31, no. 7, pp. 4755 – 4765, Jul. 2016.

[6] A. Hassanpoor, A. Roostaei, S. Norrga, M. Lindgren, "Optimization-Based Cell Selection Method for Grid-Connected Modular Multilevel Converters," *IEEE Trans. on Power Electron.*, vol.31, no.4, pp. 2780 – 2790, July 2016.

[7] M. Vasiladiotis, N. Cherix, and A. Rufer, "Accurate Capacitor Voltage Ripple Estimation and Current Control Considerations for Grid-Connected Modular Multilevel Converters," *IEEE Trans. on Power Electron.*, vol. 29, no.9, pp. 4568 – 4579, Sept. 2014.

[8] J. Mei, B. Xiao, K. Shen, L.M Tolbert, J.Y Zheng, "Modular Multilevel Inverter with New Modulation Method and Its Application to Photovoltaic Grid-Connected Generator," *IEEE Trans. on Power Electron.*, vol.28, no.11, pp. 5063 – 5073, Nov. 2013.

[9] R. Vidal-Albalade, H. Beltran, A. Rolán, E. Belenguer, R. Peña, and R. Blasco-Gimenez, "Analysis of the Performance of MMC Under Fault Conditions in HVDC-Based Offshore Wind Farms," *IEEE Trans. on Power Delivery*, vol.31, no.2, pp. 839 – 847, 2016.

[10] M. Wang, Y. Hu, W. Zhao, Y. Wang, and G. Chen, "Application of modular multilevel converter in medium voltage high power permanent magnet synchronous generator wind energy conversion systems," *IET Renewable Power Generation*, vol. 10, no. 6, pp. 824 – 833, Jun. 2016.

[11] A. Edpuganti, and A.K. Rathore, "Optimal Pulsewidth Modulation for Common-Mode Voltage Elimination of Medium-Voltage Modular Multilevel Converter fed Open-end Stator Winding Induction Motor Drives," *IEEE Trans on Ind. Electron.*, PP (99), DOI: 10.1109/TIE.2016.2586678, 2016.

[12] B. Zhao, Q. Song, J. Li, Y. Wang, and W. Liu, "High-Frequency-Link Modulation Methodology of DC-DC Transformer Based on Modular Multilevel Converter for HVDC Application: Comprehensive Analysis and Experimental Verification," *IEEE Trans. on Power Electron*, DOI: 10.1109/TPEL.2016.2586196.

[13] T. Soong and P.W. Lehn, "Internal Power Flow of a Modular Multilevel Converter with Distributed Energy Resources," *IEEE Jour. of Emerging and Selected Topics in Power Electron.*, vol.2, no. 4, pp. 1127 – 1138, Dec. 2014.

[14] G. Liu, Z. Xu, Y. Xue, and G. Tang, "Optimized Control Strategy Based on Dynamic Redundancy for the Modular Multilevel Converter," *IEEE Trans. on Power Electron.*, vol. 30, no. 1, pp. 339 – 348, Jan. 2015.

[15] B.S. Riar, T. Geyer, and U.K Madawala, "Model Predictive Direct Current Control of Modular Multilevel Converters: Modeling, Analysis, and Experimental Evaluation," *IEEE Trans. on Power Electron.*, vol.30, no.1, pp. 431 – 439, Jan. 2015.

[16] J. Xu, C. Zhao, W. Liu, and C. Guo, "Accelerated Model of Modular Multilevel Converters in PSCAD/EMTDC," *IEEE Trans. on Power Delivery*, vol.28, no.1, pp. 129 – 136, Nov. 2013.

[17] J. Xu, A.M. Gole, and C. Zhao, "The Use of Averaged-Value Model of Modular Multilevel Converter in DC Grid," *IEEE Trans. on Power Delivery*, vol.30, no.2, pp. 519 – 528, Apr. 2015.

[18] J. Wang, R. Burgos, and D. Boroyevich, "Switching-Cycle State-Space Modeling and Control of the Modular Multilevel Converter," *IEEE Journal of Emerging and Selected Topics in Power Electronics*, vol.2, no.4, pp. 1159 – 1170, Dec. 2014.

[19] F. Yu, W. Lin, X. Wang, and D. Xie, "Fast Voltage-Balancing Control and Fast Numerical Simulation Model for the Modular Multilevel Converter," *IEEE Trans. on Power Delivery*, vol.30, no.1, pp. 220 – 228, Feb. 2015.

[20] A. Korn, M. Winkelkemper, and P. Steimer, "Low output frequency operation of the Modular Multi-Level Converter," in *Proc. IEEE Energy Conversion Congress and Exposition (ECCE)*, pp. 3993–3997, Sept. 2010.

[21] A. Antonopoulos, L. Ångquist, S. Norrga, K. Ilves, L. Harnefors, and H-P. Nee, "Modular Multilevel Converter AC Motor Drives With Constant Torque From Zero to Nominal Speed," *IEEE Trans. on Industry Applications*, vol. 50, no.3, pp. 1982 – 1993, Jun. 2014.

[22] S. Debnath, J. Qin, and M. Saeedifard, "Control and Stability Analysis of Modular Multilevel Converter under Low-Frequency Operation," *IEEE Trans. on Ind. Electron.*, vol. 62, no. 9, pp. 5329 – 5339, Sep. 2015.

[23] J. Kolb, F. Kammerer, M. Gommringer, and M. Braun, "Cascaded control system of the modular multilevel converter for feeding variable speed drives," *IEEE Trans. on Power Electron.*, vol. 30, no. 1, pp. 349–357, 2015.

[24] M. Spichartz, V. Staudt, and A. Steimel, "Analysis of the module-voltage fluctuations of the modular multilevel converter at variable speed drive applications," in *Proc. IEEE International Conference on Optimization of Electrical and Electronic Equipment (OPTIM)*, pp. 751–758, May 2012.

[25] M. Pahlevaninezhad, P. Das, J. Drobnik, P. K. Jain, A. Bakhshai, "A New Control Approach Based on the Differential Flatness Theory for an AC/DC Converter Used in Electric Vehicles," *IEEE Trans. on Power Electron.*, vol. 27, no. 4, pp. 2085–2103, 2012.

[26] P. Thounthong and S. Pierfederici, "A new control law based on the differential flatness principle for multiphase interleaved DC-DC converter," *IEEE Trans. Circuits Syst. II: Exp. Briefs*, vol. 57, no. 11, pp. 903–907, Nov. 2010.

[27] E. Song, A. F. Lynch, and V. Dinavahi, "Experimental validation of a flatness-based control for a voltage source converter," in *Proc. Amer. Control Conf.*, pp. 6049–6054, Jul. 9–13, 2007.

[28] M. Fliess, J. Levine, P. Martin, and P. Rouchon, "Flatness and defect of nonlinear systems: Introductory theory and examples," *CAS Internal Report A-284*, Jan. 1994.

BIOGRAPHIES



Majid Mehrasa received the B.Sc. and M.Sc. degrees in Electrical Engineering from University of Mazandaran, Babol, Iran, in 2006 and 2009, respectively. He is currently a PhD student at the University of Beira Interior, Covilhã, Portugal. His research interests include application of nonlinear control theories into multilevel converters, distributed generation, active power filter and microgrid operation.



Edris Pouresmaeil (M'14-SM'17) received the B.Sc. and M.Sc. degrees in Electrical Engineering from University of Mazandaran, Babol, Iran, in 2003 and 2005, respectively. He received the Ph.D. degree in Electrical Engineering with honor from the Technical University of Catalonia, Barcelona Tech. (UPC), Barcelona, Spain, in 2012. After his Ph.D. he joined the Department of Electrical & Computer Engineering, at University of Waterloo, ON, Canada, as a Postdoctoral Research Fellow, and later he joined the Department of Electromechanical Engineering, at University of Beira Interior, Portugal. He is currently a Researcher with the INESC-ID, Lisbon, Portugal. His research interests include power electronics converters for distributed generation, microgrids operation, integration of renewable energies in smart grids and energy hub management system.



Shamsodin Taheri obtained his B.Sc. degree in electrical engineering from the University of Mazandaran, Iran in 2006 and completed a Master degree in 2009 at Iran University of Science and Technology (IUST). He obtained a Ph.D. degree in electrical engineering at the Université du Québec à Chicoutimi (UQAC), Canada in 2013. From 2013 to 2014, He worked at Saskpower (Technical Services & Research department), Saskatchewan, Canada. Since 2014 he has been an assistant professor at Université du Québec en Outaouais, Gatineau, Qc, Canada. His main research interests include power systems, renewable energy, high voltage, numerical modeling and transformers.



Ionel Vechiu (M'08) received the Engineer degree in electrical engineering from Galati University, Romania, in 2001 and his M.S. and Ph.D. degrees from the University of Le Havre, France, in 2002 and 2005, respectively. In 2013, he received the HDR in Applied Power Electronics and Control from Grenoble INP, France. He is currently Professor at ESTIA Institute of Technology, France and his research interests include the power electronics applied to renewable energy conversion and storage, dynamic modelling & simulation of electric power systems, including control strategies for distributed generation integration into weak grids.



João P. S. Catalão (M'04-SM'12) received the M.Sc. degree from the Instituto Superior Técnico (IST), Lisbon, Portugal, in 2003, and the Ph.D. degree and Habilitation for Full Professor ("Agregação") from the University of Beira Interior (UBI), Covilha, Portugal, in 2007 and 2013, respectively.

Currently, he is a Professor at the Faculty of Engineering of the University of Porto (FEUP), Porto, Portugal, and Researcher at INESC TEC, INESC-ID/IST-UL, and C-MAST/UBI. He was the Primary Coordinator of the EU-funded FP7 project SiNGULAR ("Smart and Sustainable Insular Electricity Grids Under Large-Scale Renewable Integration"), a 5.2-million-euro project involving 11 industry partners. He has authored or coauthored more than 550 publications, including 185 journal papers (more than 50 IEEE Transactions/Journal papers), 325 conference proceedings papers, 31 book chapters, and 14 technical reports, with an h-index of 34 and over 4500 citations (according to Google Scholar), having supervised more than 50 post-docs, Ph.D. and M.Sc. students. He is the Editor of the books entitled *Electric Power Systems: Advanced Forecasting Techniques and Optimal Generation Scheduling* and *Smart and Sustainable Power Systems: Operations, Planning and Economics of Insular Electricity Grids* (Boca Raton, FL, USA: CRC Press, 2012 and 2015, respectively). His research interests include power system operations and planning, hydro and thermal scheduling, wind and price forecasting, distributed renewable generation, demand response and smart grids.

Prof. Catalão is an Editor of the IEEE TRANSACTIONS ON SMART GRID, an Editor of the IEEE TRANSACTIONS ON SUSTAINABLE ENERGY, an Editor of the IEEE TRANSACTIONS ON POWER SYSTEMS, and an Associate Editor of the *IET Renewable Power Generation*. He was the Guest Editor-in-Chief for the Special Section on "Real-Time Demand Response" of the IEEE TRANSACTIONS ON SMART GRID, published in December 2012, and the Guest Editor-in-Chief for the Special Section on "Reserve and Flexibility for Handling Variability and Uncertainty of Renewable Generation" of the IEEE TRANSACTIONS ON SUSTAINABLE ENERGY, published in April 2016. Since May 2017, he is the Corresponding Guest Editor for the Special Section on "Industrial and Commercial Demand Response" of the IEEE TRANSACTIONS ON INDUSTRIAL INFORMATICS. He was the recipient of the 2011 Scientific Merit Award UBI-FE/Santander Universities and the 2012 Scientific Award UTL/Santander Totta, in addition to an Honorable Mention in the 2017 Scientific Awards ULisboa/Santander Universities. Moreover, he has won 4 Best Paper Awards at IEEE Conferences.